A C_8P monolayer with cross-sp-hybridized phosphorus atom and ultrahigh energy density as a K-ion battery anode

Xu Yan[1], Sheng Wang[1], Shicong Ding[1], Javed Rehman[2,*], Yong Liu, and Guochun Yang[1,3*]

[1]*State Key Laboratory of Metastable Materials Science & Technology and Key Laboratory for Microstructural Material Physics of Hebei Province, School of Science, Yanshan University, Qinhuangdao 066004, China*

[2]*State Key Laboratory of Metastable Materials Science and Technology, School of Materials Science and Engineering, Yanshan University, Qinhuangdao 066004, China*

[3]*Centre for Advanced Optoelectronic Functional Materials Research and Key Laboratory for UV Light-Emitting Materials and Technology of Northeast Normal University, Changchun 130024, China*

Index **page**

Computational Details

The particle swarm optimization (PSO) method within the evolutionary algorithm as implemented in the Crystal structure Analysis by Particle Swarm Optimization (CALYPSO) code[1,2] was employed to find the lowest energy structures of $C_xP_yN_z$ (x = 1~16, y = 1~4, and z = 0~2) monolayers. Unit cells containing 1 and 2 formula units (f.u.) with buckled and planar structures were considered. In the first step, random structures with certain symmetry were constructed in which atomic coordinates were generated by the crystallographic symmetry operations. Local optimizations using the VASP code[3] were done with the conjugate gradients method and stopped when Gibbs free energy changes became smaller than 1×10^{-6} eV per cell. After processing the first-generation structures, 60% of them with lower enthalpies were selected to construct the next generation structures by Particle Swarm Optimization (PSO). 40% of the structures in the new generation were randomly generated. A structure fingerprinting technique of bond characterization matrix was applied to the generated structures, so that identical structures were strictly forbidden. These procedures significantly enhance the diversity of the structures, which is crucial for structural global search efficiency. In most cases, structural searching simulations for each calculation were stopped after generating 500 ~ 600 structures (e.g., about 10 ~ 15 generations).

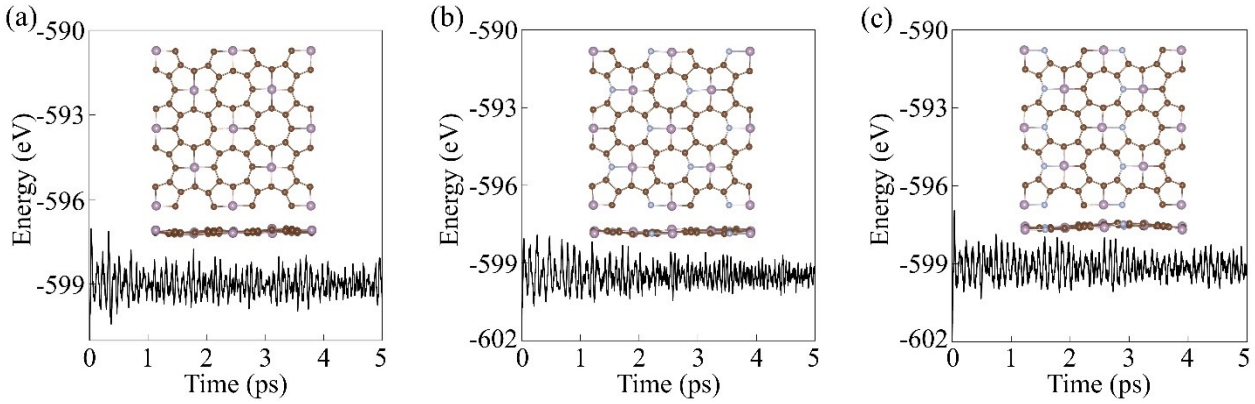

Fig. S1 AIMD simulations of the (a) C_8P, (b) α-C_7PN, and (c) β-C_7PN monolayers at 300 K.

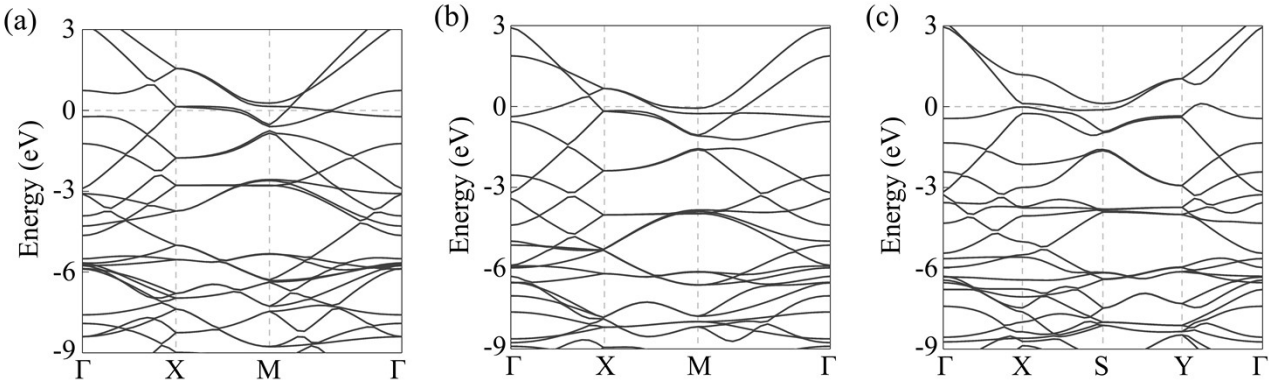

Fig. S2 Band structures of the (a) C_8P, (b) α-C_7PN, and (c) β-C_7PN monolayers at HSE06 level.

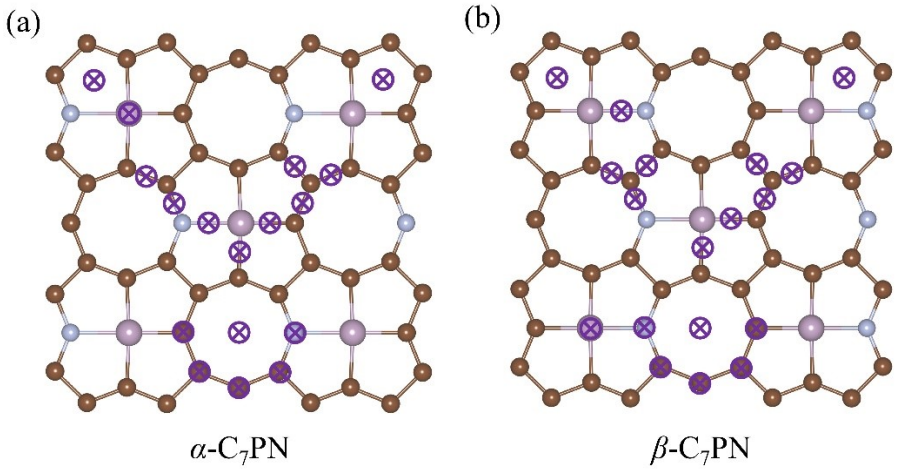

Fig. S3 Possible adsorption sites of Li/Na/K on the (a) α-C_7PN and (b) β-C_7PN monolayers.

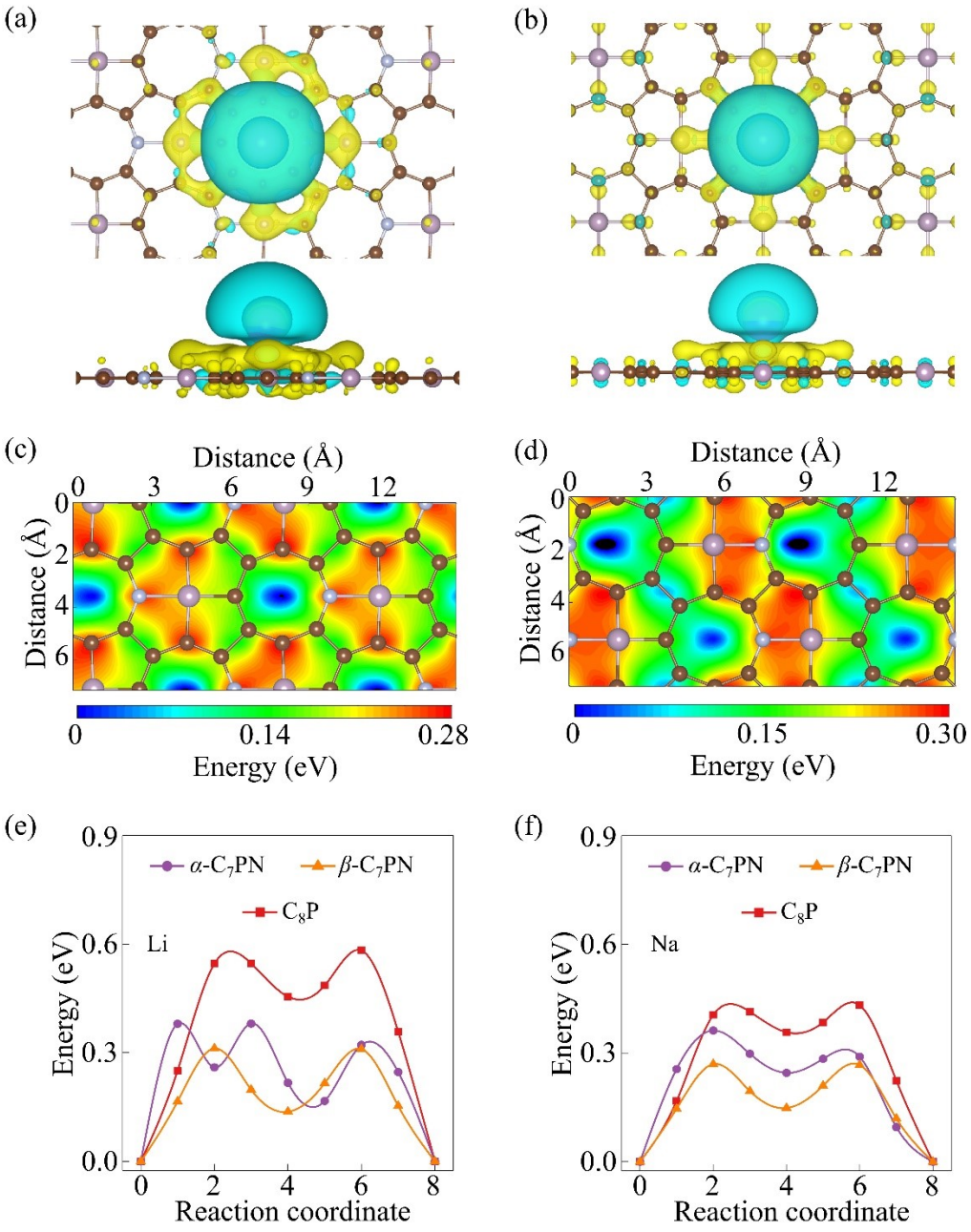

Fig. S4 Charge density difference of K adsorbed on the (a) α-C_7PN and (b) β-C_7PN monolayers. Local maps of the scanning potential energy surface of the (c) α-C_7PN and (d) β-C_7PN monolayers. Diffusion barrier energy of (e) Li and (f) Na migration on the C_8P, α-C_7PN, and β-C_7PN monolayers.

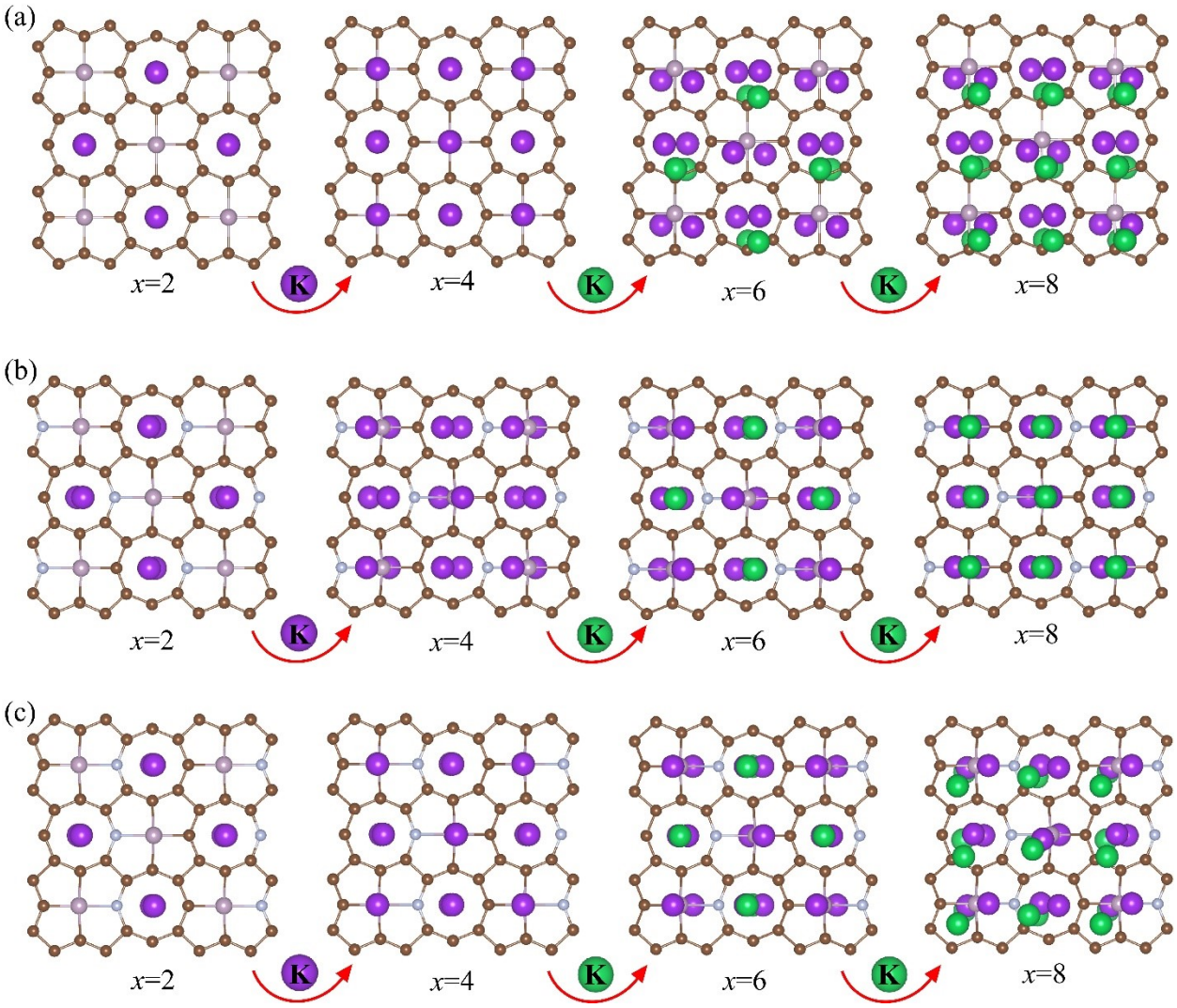

Fig. S5 Top/bottom K loading on the (a) C_8P, (b) α-C_7PN, and (c) β-C_7PN monolayers.

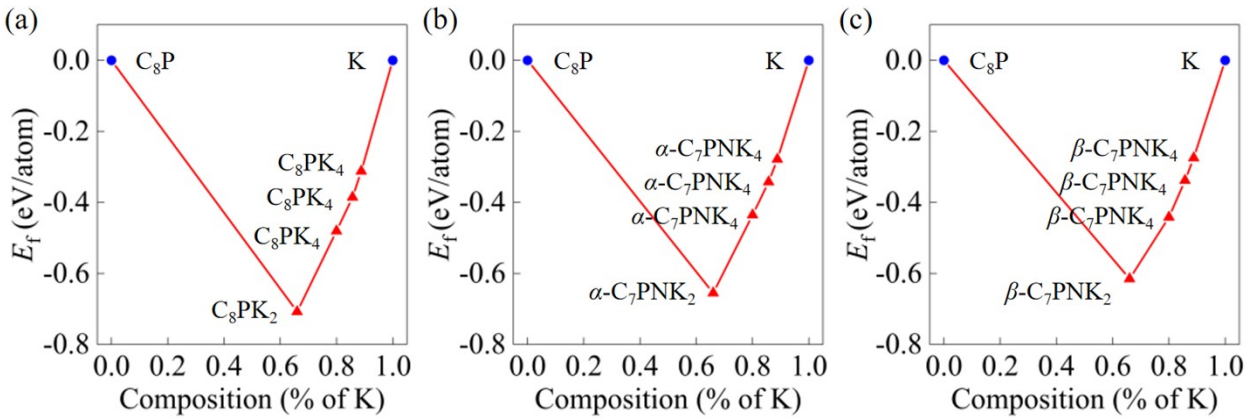

Fig. S6 Relative stability of (a) C_8PK_x, (b) α-C_7PNK_x, and (c) β-C_7PNK_x ($x = 2, 4, 6, 8$) with respect to an elemental solid K and the C_8P/α-C_7PN/β-C_7PN monolayer at 0 K. The optimized monolayers corresponding to the data points located on the convex hull are thermodynamically stable.

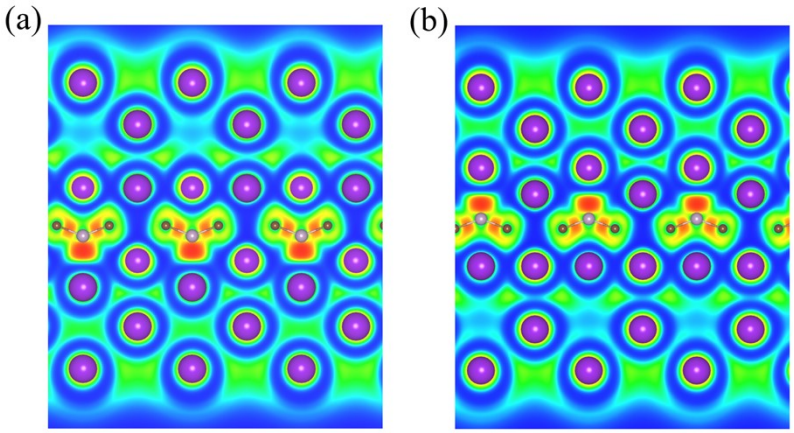

Fig. S7 ELF snapshots of K loaded on the (a) α-C_7PN and (c) β-C_7PN monolayers.

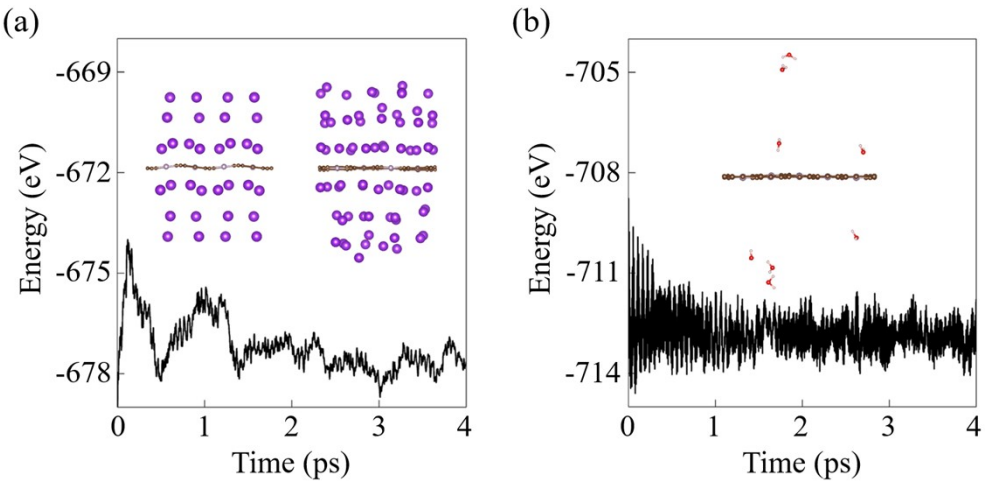

Fig. S8 (a) AIMD simulations of C_8PK_8 at 300 K. (b) AIMD simulations of the C_8P monolayer in an aqueous environment at 300 K.

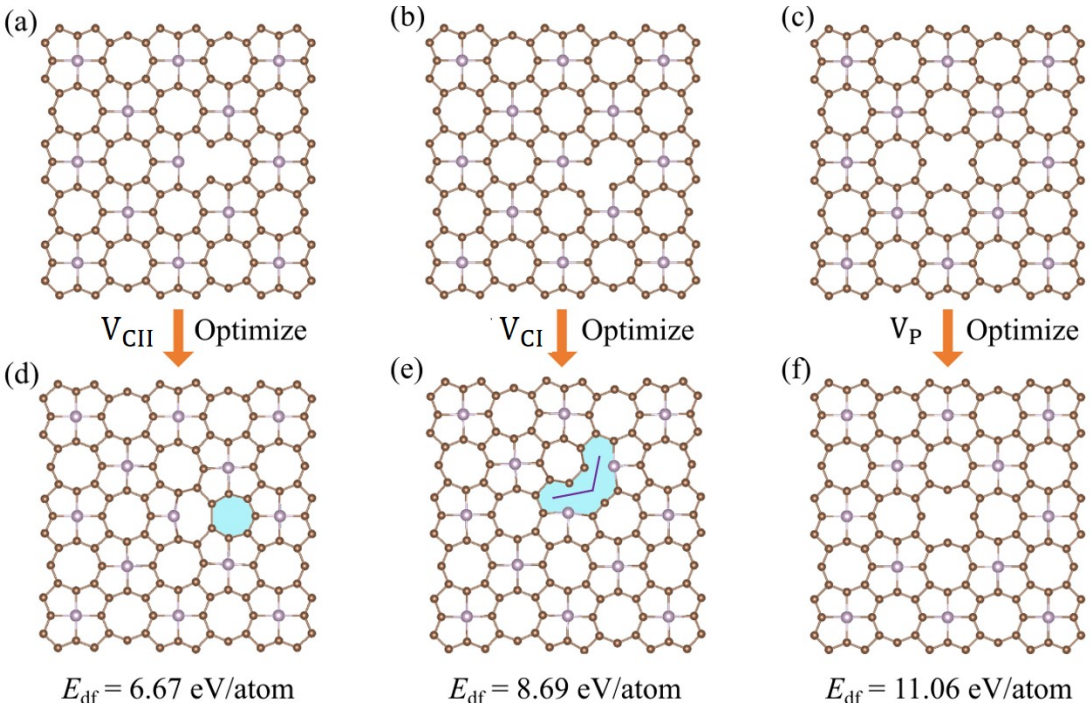

Fig. S9 (a-c) The constructed and (d-f) the optimized structures of C_8P containing a single C vacancy (V_{CII} and V_{CI}) and P vacancy (V_P) .

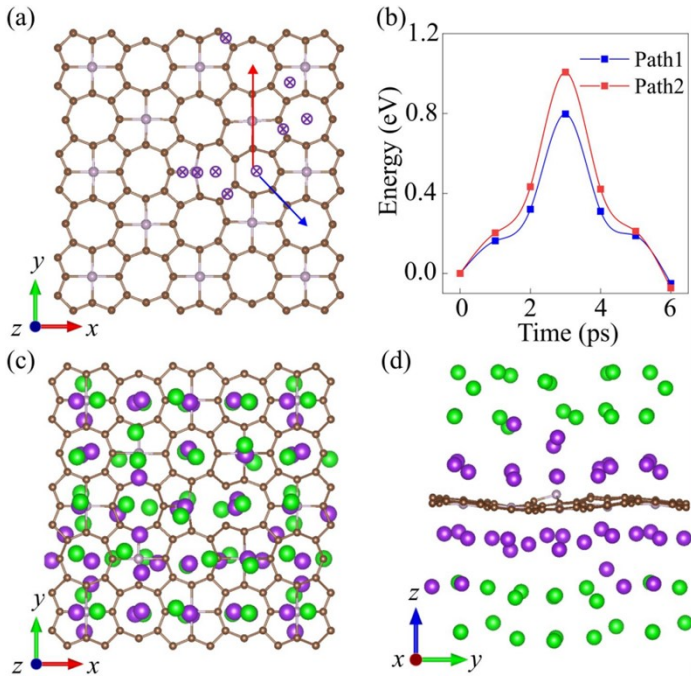

Fig. S10 (a) Considered K absorption site and migration paths of the C_8P monolayer with $^{V_{CII}}$. (b) Diffusion energy barriers of K migration on the defective C_8P monolayer. (c and d) Top and side views of the C_8PK_8 with $^{V_{CII}}$.

Table S1 Structural parameters of the C_8P monolayer obtained from PBE functional, lattice parameters in bracket are obtained with the PBEsol functional.

	Lattice Parameters (Å, °)	**Atoms**	**Positions (fractional)** *x*	*y*	*z*
C_8P	a = 7.313(7.298)	C	0.3301	0.0000	0.5000
	b = 7.313(7.298)	C	0.7589	0.8216	0.5000
	c = 20.9283	C	0.7589	0.1784	0.5000
	$\alpha = \beta = \gamma =$	C	0.9021	0.3216	0.5000
	90.0000	C	0.9021	0.6784	0.5000
		C	0.0805	0.7504	0.5000
		C	0.0805	0.2496	0.5000
		C	0.8301	0.5000	0.5000
		C	0.2589	0.3216	0.5000
		C	0.2589	0.6784	0.5000
		C	0.4021	0.8216	0.5000
		C	0.4021	0.1783	0.5000
		C	0.5802	0.2504	0.5000
		C	0.5802	0.7496	0.5000
		C	0.8309	0.0000	0.5000
		C	0.3309	0.5000	0.5000
		P	0.0805	0.0000	0.5000
		P	0.5805	0.5000	0.5000

Table S2 Structural parameters of the α-C_7PN monolayer obtained from PBE functional, lattice parameters in bracket are obtained with the PBEsol functional.

	Lattice Parameters (Å, °)	**Atoms**	**Positions (fractional)**		
			x	***y***	***z***
***α*-C_7PN**	a = 7.330(7.311)	C	0.3300	0.0000	0.5000
	b = 7.174(7.161)	C	0.7585	0.8240	0.5000
	c = 20.9283	C	0.7585	0.1760	0.5000
	$\alpha = \beta = \gamma =$	C	0.9013	0.3193	0.5000
	90.0000	C	0.9013	0.6807	0.5000
		C	0.0794	0.7504	0.5000
		C	0.0794	0.2496	0.5000
		C	0.8298	0.5000	0.5000
		C	0.2585	0.3240	0.5000
		C	0.2585	0.6760	0.5000
		C	0.4013	0.8193	0.5000
		C	0.4013	0.1807	0.5000
		C	0.5793	0.2504	0.5000
		C	0.5793	0.7496	0.5000
		P	0.8880	0.0000	0.5000
		P	0.5888	0.5000	0.5000
		N	0.8277	0.0000	0.5000
		N	0.3277	0.5000	0.5000

Table S3 Structural parameters of the β-C_7PN monolayer obtained from PBE functional, lattice parameters in bracket are obtained with the PBEsol functional.

	Lattice Parameters (Å, °)	**Atoms**	**Positions (fractional)**		
			x	***y***	***z***
***β*-C_7PN**	a = 7.312(7.294)	C	0.9294	0.5728	0.5000
	b = 7.178(7.164)	C	0.0706	0.0728	0.5000
	c = 20.9283	C	0.5715	0.5707	0.5000
	$\alpha = \beta = \gamma =$	C	0.4285	0.0707	0.5000
	90.0000	C	0.7529	0.5003	0.5000
		C	0.2471	0.0000	0.5000
		C	0.9294	0.9272	0.5000
		C	0.0706	0.4272	0.5000
		C	0.5715	0.9293	0.5000
		C	0.4285	0.4293	0.5000
		C	0.4995	0.7500	0.5000
		C	0.5005	0.2500	0.5000
		C	0.7529	0.0000	0.5000
		C	0.2472	0.5000	0.5000
		P	0.7468	0.2500	0.5000
		P	0.2532	0.7500	0.5000
		N	0.0019	0.7500	0.5000
		N	-0.0019	0.2500	0.5000

Table S4 Bond lengths in the C_8P, α-C_7PN, and β-C_7PN monolayers.

Bond length (Å)	C_8P	α-C_7PN	β-C_7PN
C-C	1.41~1.48	1.40~1.47	1.39~1.47
C-P	1.83	1.77~1.79	1.80
C-N		1.36	1.38
P-N		1.91	1.83

Table S5 Elastic constants of the C_8P, α-C_7PN, and β-C_7PN monolayers.

Parameters (N/m)	C_8P	α-C_7PN	β-C_7PN
C_{11}	303.233	295.228	300.164
C_{12}	58.461	77.596	74.079
C_{66}	129.025	132.263	132.487

Table S6 Lattice parameters (Å) of the C_8PK_x, α-C_7PNK_x, and β-C_7PNK_x (x = 2, 4, 6, and 8).

Phase	x = 2	x = 4	x = 6	x = 8
C_8PK_x	a = 7.35	a = 7.39	a = 7.39	a = 7.39
	b = 7.39	b = 7.40	b = 7.39	b = 7.38
α-C_7PNK_x	a = 7.45	a = 7.45	a = 7.44	a = 7.44
	b = 7.14	b = 7.14	b = 7.15	b = 7.14
β-C_7PNK_x	a = 7.37	a = 7.43	a = 7.43	a = 7.43
	b = 7.22	b = 7.17	b = 7.16	b = 7.15

References

1. Y. Wang, J. Lv, L. Zhu and Y. Ma, *Comput. Phys. Commun.*, 2012, **183**, 2063-2070.
2. Y. Wang, J. Lv, L. Zhu and Y. Ma, *Phys. Rev. B*, 2010, **82**, 094116.
3. G. Kresse and J. Furthmùller, *Phys. Rev. B*, 1996, **54**, 11169.